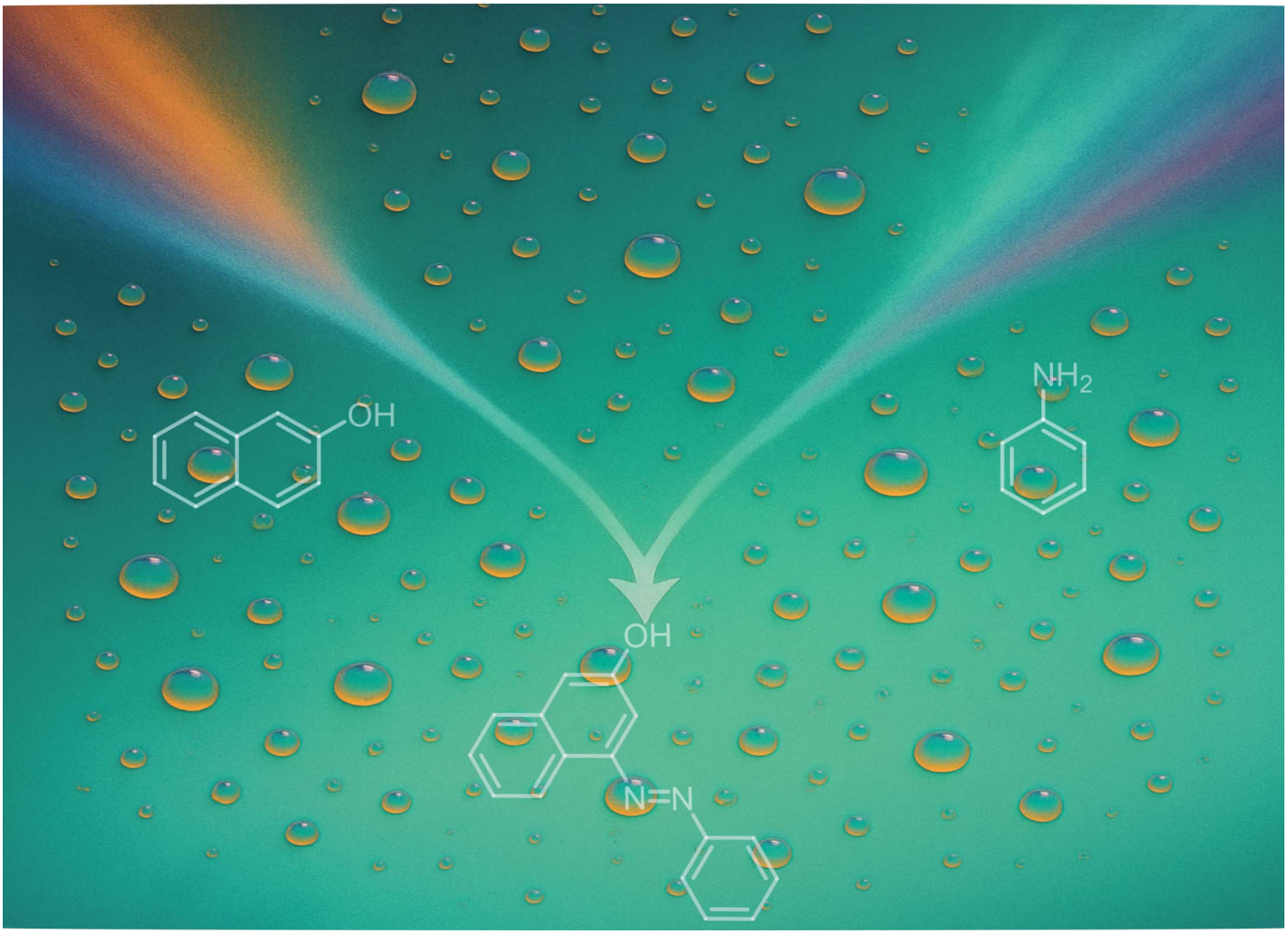

Showcasing research from Dr Hessam Mehr's laboratory, School of Chemistry, University of Glasgow, Scotland, UK.

Programmable aerosol chemistry coupled to chemical imaging establishes a new arena for automated chemical synthesis and discovery

Aerosol microdroplets are gaining attention as inherently parallel media for chemical reactions, but harnessing their full potential requires revisiting the fundamentals of synthetic chemistry. How will syntheses be conceived and executed in this new arena, and what toolbox of analytical techniques is suited to the challenge of interrogating vast inhomogeneous reactivity outcomes? In this work, we set out a framework, enabled by open programmable hardware, microscopy and machine vision, that opens up a pathway for translating traditional synthesis and discovery methodology for execution in aerosol microdroplets.

Image reproduced by permission of Hessam Mehr and Zehua Li from *Digital Discovery*, 2025, **4**, 2423.

Created with the use of Microsoft Copilot.

As featured in:

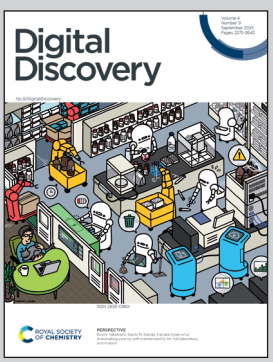

See S. Hessam M. Mehr *et al.*, *Digital Discovery*, 2025, **4**, 2423.

ROYAL SOCIETY OF CHEMISTRY

rsc.li/digitaldiscovery

Registered charity number: 207890

Digital Discovery

ROYAL SOCIETY OF CHEMISTRY

PAPER

View Article Online
View Journal | View Issue

Cite this: *Digital Discovery*, 2025, **4**, 2423

Programmable aerosol chemistry coupled to chemical imaging establishes a new arena for automated chemical synthesis and discovery†

Jakub D. Wosik,‡ Chaoyi Zhu,‡ Zehua Li and S. Hessam M. Mehr *

Aerosols have emerged as a massively parallel reaction medium promising accelerated reactivity and unanticipated reactivity outcomes, yet exploration of these properties has so far only been confined to specific reactions. Wider deployment in chemical synthesis and discovery is impeded by the lack of a general-purpose formalism for conceiving multi-step chemical transformations in the aerosol medium and standardised building blocks to enable adaptation of existing synthesis procedures to execution in the inherently stochastic and inhomogeneous aerosol phase. Here we propose a framework based on programmable timed release of reagents as atomised solutions that provides the minimum necessary building blocks for synthesis in an automated aerosol reactor. This framework both connects synthesis in traditional bulk media with aerosols and lays the foundation for massively parallel discovery in airborne microdroplets. To validate our proposed formalism with a concrete methodology, we demonstrate a prototype open hardware platform and three examples of automated procedures. Further, we propose chemical imaging as a category of analytical methodology tailored to interrogation of aerosols. As a proof-of-principle demonstration, we use optical microscopy to detect reactivity in the resulting microdroplets and study the spatial distribution of their compositions in response to changes in the synthesis program.

Received 10th March 2025
Accepted 8th July 2025

DOI: 10.1039/d5dd00100e

rsc.li/digitaldiscovery

Introduction

Research at the interface of chemistry and aerosol science has intensified in recent years, sparked initially by observation of unusual or accelerated reactivity in electrosprays.[1–5] Chemical reactivity within aerosol microdroplets as a microscopic reaction vessel is rapidly generating research interest with a host of potential advantages over bulk media. Results published so far have reported a dramatic departure from bulk reactivity outcomes,[6–8] signalling the possibility both of reaction acceleration and modulating selectivity for different products. From a green chemistry perspective, aerosol experiments offer a drastic reduction in reaction volumes and hence waste, invaluable especially in the reaction discovery and optimisation stages where wide combinations of reagents, stoichiometries and reaction conditions need to be explored. The large surface to volume ratio of aerosols facilitates rapid solvent evaporation and/or exchange,[9] replacing lengthy evaporation and resuspension steps on the benchtop. For researchers wishing to advance the conceptual underpinnings of experimental chemistry, aerosols are inherently high throughput and stochastic reaction media, dovetailing with the growing use of large datasets in chemistry. As reaction systems, they are readily amenable to direct interrogation using microscopy[10] and mass spectrometry. The full potential of aerosols as a venue for chemical reactions is not yet fully understood,[11] though parallels may be drawn to flow chemistry, whose unique affordances—augmenting traditional synthesis with a spatial dimension—have redefined synthetic chemical methodology.[12]

Studies on chemical reactivity within aerosols have so far been performed in the steady state,[3,13,14] often using pre-mixed reactants,[15] and predominantly on aerosol particles formed *via* electrospray ionisation (ESI) with mass spectrometric detection of products at trace concentrations.[16] There are particular gaps regarding applicability to more complex, multi-step transformations; the contribution of atomisation *versus* ESI charging to the observed reactivity; and analytical workflows capable of interrogating the inhomogeneous nature of aerosol particles as individual microreactors. Here, we endeavour to tackle all three of these extant challenges. We present a general experimental framework for time-resolved synthesis and discovery in the aerosol phase, implemented within a standard programmable open-hardware setup which does not depend on ESI, coupled to microscopy and computational image analysis as a means of probing the spatial diversity of reactivity outcomes.

School of Chemistry, University of Glasgow, Advanced Research Centre, 11 Chapel Lane, Glasgow G11 6EW, UK. E-mail: Hessam.Mehr@glasgow.ac.uk

† Electronic supplementary information (ESI) available. See DOI: https://doi.org/10.1039/d5dd00100e

‡ Equal contribution.

Table 1 Subset of laboratory synthesis operations mirrored in our aerosol-based experimental framework

Phase	Bulk synthesis operation	Aerosol synthesis correspondence
Reaction	Reagent addition Mixing	Timed aerosol release Intersecting aerosol jets
Isolation	Evaporation Filtration (to remove solvent)	Droplet evaporation Droplet evaporation
Analysis	LC-MS, NMR, *etc.* Yield and purity	Microscopy, imaging mass spectrometry Composition statistics of final droplets

The physical operations used within our framework are inspired by common laboratory manipulations used in batch chemical synthesis, for a subset of which we have developed aerosol phase equivalents, Table 1. Specifically, the bulk addition of reagents is mirrored by their release as aerosols; control of stoichiometry by measuring weight/volume is instead achieved *via* the length and intensity of aerosol pulses, interspersed with time delays during which reactions are allowed to progress; and bulk mixing *via* stirring is replaced with the generation of mixed microdroplets resulting from collisions between intersecting aerosol jets.

Establishing a direct one-to-one equivalence may not always be straightforward or even desirable. Filtering bulk suspensions to recover solids is not only challenging to implement in microdroplets, but often unnecessary due to the rapid equilibration of aerosol microdroplets with their surrounding environment. Likewise, bulk analytical techniques like NMR or LC-MS are optimised for interrogation of homogeneous reaction mixtures, as opposed to aerosol microdroplets heterogeneous chemical packets with a wealth of collective reactivity information. Finally, the high surface-to-volume ratio of aerosol microdroplets complicates independent control of temperature and vapour pressure/relative humidity due to rapid equilibration. Consequently, this initial formulation does not include explicit temperature adjustment operations paralleling heating/cooling/reflux in traditional chemistry.

Results

The two-step synthesis of the azo dye Sudan I can be used as a simple example of translating bulk synthesis to aerosol-phase operations. The bulk synthesis protocol relies on conversion of aniline to a diazonium intermediate followed by azo coupling involving the conjugate base of β-naphthol, Fig. 1A. The incompatible nature of reaction conditions for these transformations—acidic, followed by basic—necessitates two distinct reaction steps.

Translating the bulk mixing steps to aerosol release instructions initially results in the sequence in Fig. 1B, where the addition of each reagent is abstractly represented as release events on a dedicated timeline. Specifically, the initial diazotisation step between aniline and nitrous acid is equated with their simultaneous release, followed by a delay t_1, during which the diazo intermediate is allowed to form. Subsequent release of

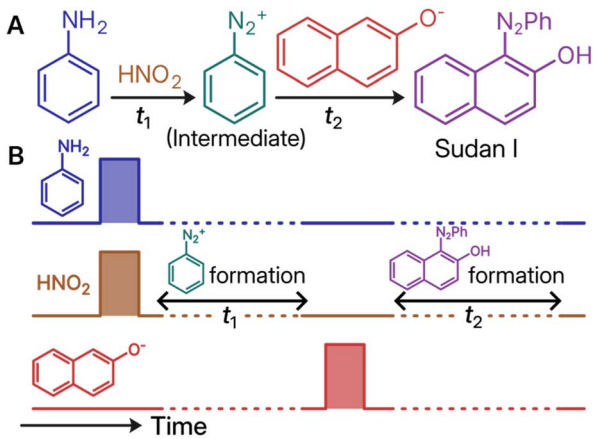

Fig. 1 Translation of procedures from traditional bulk synthesis to aerosol chemistry. (A) Example of a two-step synthetic procedure in organic chemistry, in this case leading to the azo dye Sudan I. (B) Abstract representation of the same process *via* synchronised stepwise release of reagents and delays allowing formation of intermediates.

β-naphthoxide initiates the second step and associated period t_2, ultimately resulting in the diazo product. This abstract representation clarifies the essential features of the synthesis sequences—reagents brought into contact at different points in time—without constraining the modality for achieving this.

Executing an aerosol-phase synthesis procedure based on this abstract description requires a suitable aerosol source and reactor geometry. Our investigations have targeted vibrating mesh atomisers, a chemically resistant and cost-effective aerosol source that is amenable to automation[10] and for which we have created a highly adaptable programmable hardware platform. A suitable reactor configuration requires in turn ensuring (i) there is an aerosol source for each release timeline and, (ii) that the sources involved in each mixing event are arranged in a convergent geometry to facilitate droplet coalescence, Fig. 2. In cases involving the combination of reagents and intermediates, such as the second step of synthesising Sudan I, the reagent source is aimed at a region with a large concentration of intermediate microdroplets.

For initial experimental validation of our system's ability to generate reactivity within microdroplets, we undertook benchmark reactions exploring fundamental reactivity archetypes. We chose reactants that would undergo a visible colour change

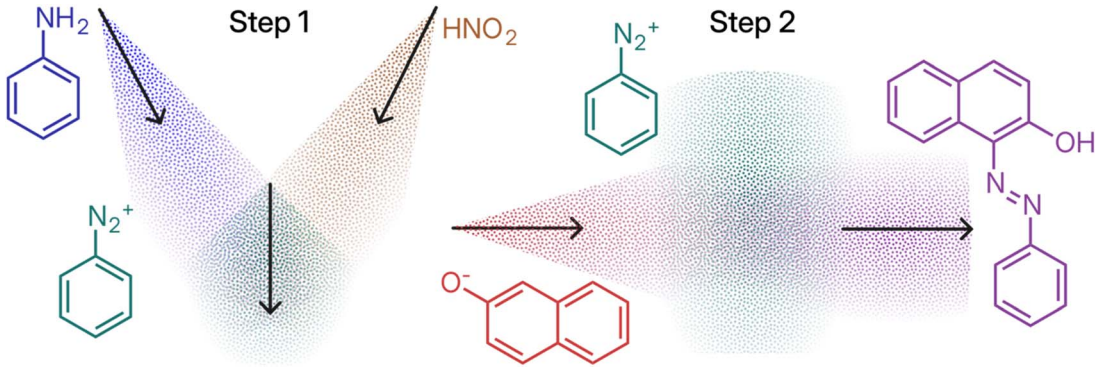

Fig. 2 Schematic implementation of the timeline for Sudan I synthesis in an aerosol setup. In the first step, aniline and nitrous acid microdroplets are combined to form the benzenediazonium intermediate, which subsequently collide with a jet of β-naphthoxide (red) aerosol, ultimately producing the Sudan I azo product.

Table 2 Basic reactivity types executed in our aerosol reactor

Reactivity type	Representative reaction	Detected colors
Acid–base	X: bromothymol blue (BTB)	X: yellow
	Y: NaOH + phenolphthalein	Y: purple product: blue
Redox	X: Ce^{4+}	X: yellow
	Y: Fe(II) ferroin	Y: red product: blue
Azo coupling	X: benzenediazonium chloride	X: colorless
	Y: sodium 2-naphtholate	Y: colorless product: red

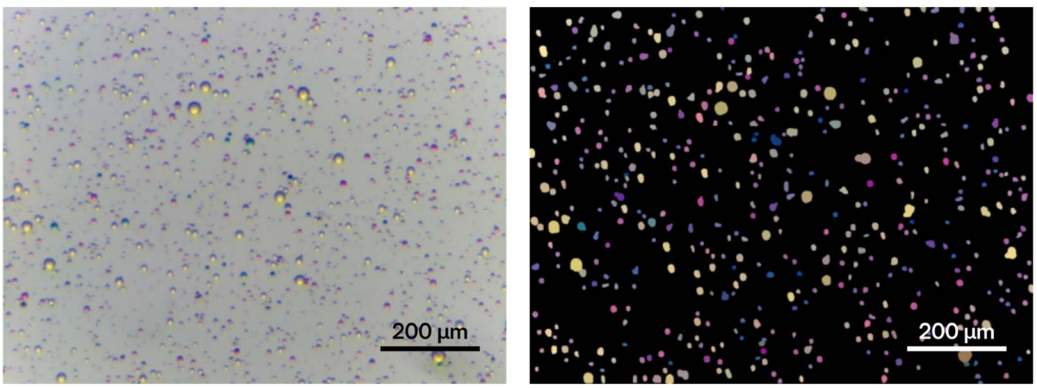

Fig. 3 Optical microscope image of collected droplets in the reaction of yellow acid and purple base microdroplets with formation of blue product droplets (left). Computational segmentation of the image with assignment of a representative colour, in this case sampled from the centre of each region (right).

upon reaction (Table 2) in order to facilitate observation of reactivity outcomes within individual droplets.

Starting with acid–base reactivity, optical microscopy of the deposited microdroplets showed evidence of both reagent solutions, along with "daughter" product microdroplets, Fig. 3, detectable based on the color change of BTB indicator from yellow to blue. Using a machine vision model (Segment Anything Model, SAM),[17] we were able to calculate a mask for individual droplets, indicating their location and size within the image. This spatial information was combined with the image to calculate a representative colour for each droplet, and the resulting colour distribution fed to a statistical mixture model capable of categorising droplets as acid, base, or product (full details in ESI†).

The same analysis applied to the redox reaction of Ce^{4+}—specifically aqueous ammonium cerium(IV) nitrate — and ferroin $[Fe(phen)_3]^{2+}$ gave a distribution of pale yellow (oxidant), red (reducing agent), and blue (oxidised ferroin product) droplets, Fig. 4.

Although the full spectral information from each droplet has been reduced to a single RGB reading, analysis of these values gives valuable insight into the distribution of chemical

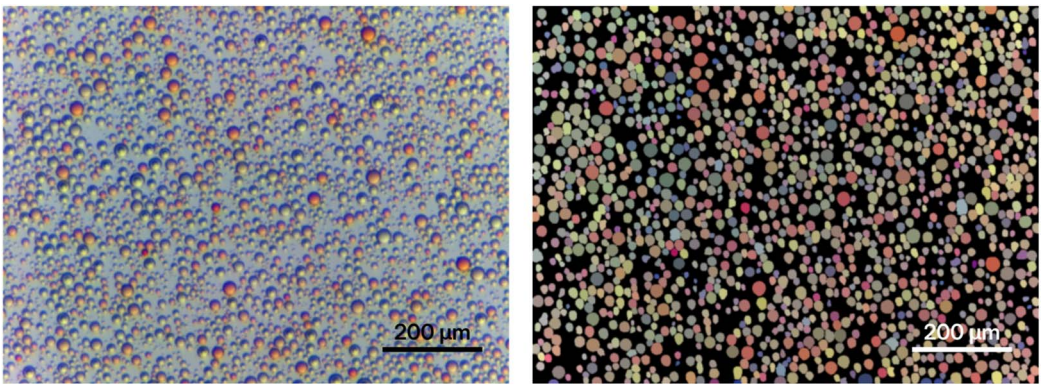

Fig. 4 Yellow Ce(IV) and red ferroin(II) microdroplets observed *via* optical microscopy along with blue ferroin(III) product (left). Computational segmentation with representative RGB sampled from the centre of each region (right).

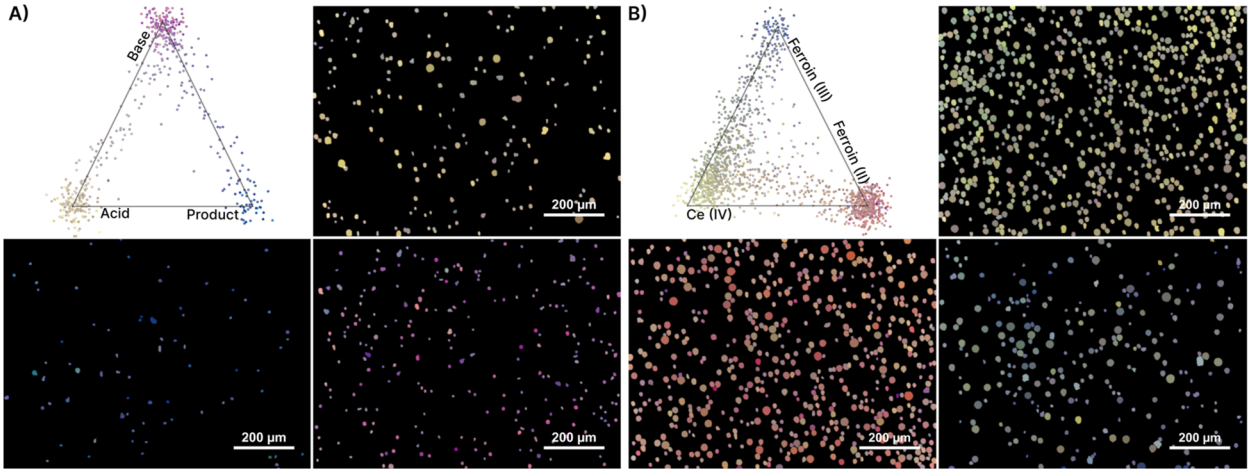

Fig. 5 Colour-based resolution of microdroplets using a Gaussian mixture model for acid–base (A) and redox (B) reactivity experiments.

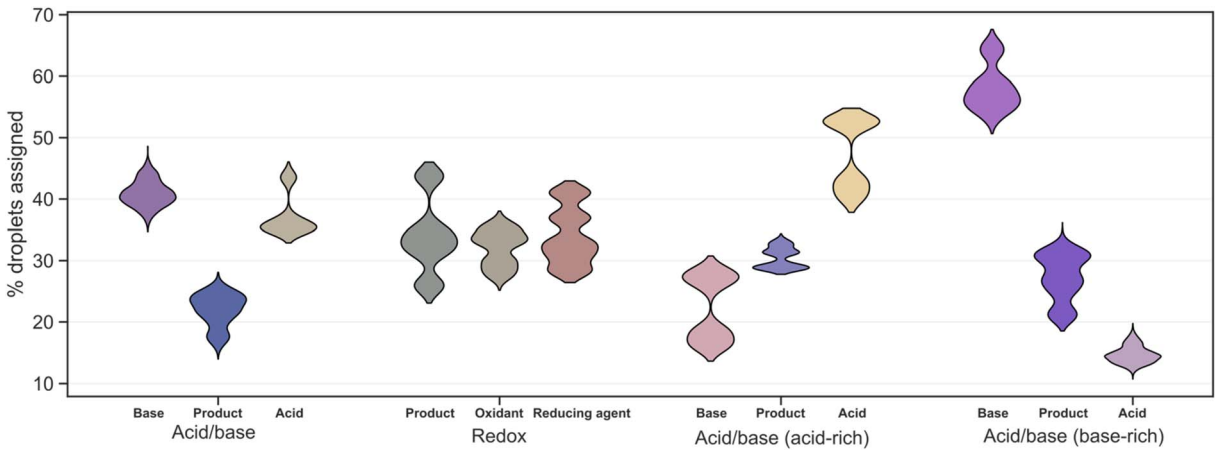

Fig. 6 Quantifying the statistical distribution of droplet assignments per sample. Each region's colour corresponds to the RGB coordinates of the mean value for the Gaussian mixture component that it represents.

composition across the sample. Using a Gaussian mixture model, for instance, not only can droplets be assigned a principal constituent (*e.g.* in the case of our redox example, Ce^{4+}, ferroin, or oxidised ferroin), their composition can be visualised on a simplex, Fig. 5. Interestingly, depending on the type of reactivity some regions appear disjoint, while others show a continuum of compositions. There is an apparent continuum of Ce^{4+} and oxidised ferroin compositions, for instance,

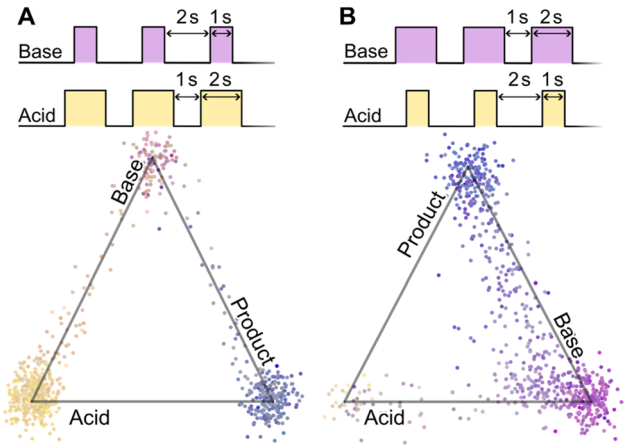

Fig. 7 Programmatic control of reaction outcomes *via* adjustment of acid and base release durations. Top diagrams represent the aerosol release program, showing the duration of acid/base release from the respective atomisers, along with intervening pauses. Longer release of acid *vs.* base in each cycle (A) leads to a larger relative population of "unreacted" yellow acid droplets relative. Longer base release pulses (B) produce a surplus of unreacted purple base droplets. The proportion of product droplets is comparable, in line with equal temporal overlap between acid and base activations (1 s per cycle) in A and B.

consistent with oxidised ferroin being likely in an oxidant-rich mixture, Fig. 5B. Similarly, the blue region corresponding to basic bromothymol blue and the purple NaOH + phenolphthalein forms a continuum, in line with the former only being visible under basic conditions, Fig. 5A.

As expected for an inherently stochastic reaction medium, outcomes in the aerosol phase are best understood in terms of distributions rather than single aggregate numbers. There is variability in droplet populations, even among different areas of the same sample, which combines with uncertainty in droplet detection and composition assignment, Fig. 6.

Droplet composition statistics can be linked to reaction inputs, namely the relative duration of aerosol release pulses as a proxy for reaction stoichiometry, opening up the possibility of steering reactivity towards desired outcomes. In an experiment aimed at demonstrating this possibility, changing the relative duration of acid and base atomiser activations led to a proportionate response in the final microdroplet populations, Fig. 6 and 7.

Finally, we attempted a qualitative synthesis of Sudan I, as an example of a two-step organic synthesis. A simplified setup using two rather than three aerosol sources was used for simplicity of implementation at this early stage. Specifically, a pre-mixed solution of aniline and nitrous acid was used in one aerosol source with a second aerosol source generating aqueous microdroplets of β-naphthoxide. Optical microscopy images showed evidence of Sudan I formation as red droplets, Fig. 8 (see ESI† for LC-MS analysis).

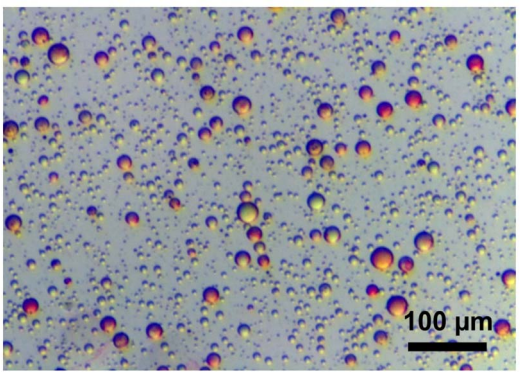

Fig. 8 Microscope image showing the formation of Sudan I (droplets) due to the reaction between benzenediazonium chloride and sodium β-naphthoxide microdroplets.

Methods

Translation of conventional synthetic chemistry to the aerosol phase required building a reactor into which reagent solutions could be introduced as aerosols. We used vibrating mesh technology as a compact, inexpensive and chemically robust option for aerosol production, combining it with our open hardware platform, dubbed AeroBoard,[18] Fig. 9A, that makes programmable aerosol chemistry possible using vibrating mesh atomisers (VMAs). Currently commercial circuitry for activating VMAs is only capable of controlling a single atomiser, lacking the programmability, synchronisation and fine control over the intensity or timing of aerosol release required in our methodology. The AeroBoard addresses this shortcoming by providing programmable, fully synchronised control of up to nine VMAs, allowing aerosolisation of multiple solutions in parallel and with arbitrary timing/dosage patterns. It integrates directly with our customisable reactor design, Fig. 9B, also released as open hardware.

The AeroBoard is implemented as a printed circuit board (PCB) that acts as a carrier for a Raspberry Pi Pico microcontroller board, which is used for programmatic control of board devices, Fig. 9. The PCB houses nine discrete piezoelectric drivers, each capable of actuating a vibrating mesh atomiser. The board can be powered *via* the Pico's 5 V USB voltage or an external power supply. Consumer VMA devices typically produce a continuous stream of aerosols *via* constant activation of the VMAs, whereas the AeroBoard uses the Pico's unique programmable I/O (PIO) system to generate a train of pulse forms, calculated according to the specific reaction sequence. Pulse generation is synchronised across all nine channels to achieve exact timing and dosing of aerosol release. The supply voltage can be adjusted to modify the intensity of the ejected aerosol jet or to overcome higher solution viscosity, and the generated oscillation frequency can be adjusted programmatically in real time to match the piezoelectric element's resonant frequency (see ESI† for full implementation details). The associated firmware and programming interface are available as open-source software, documented separately.[19]

Discussion

Here, we demonstrate for the first time a framework for chemical synthesis in the aerosol phase which is fundamentally

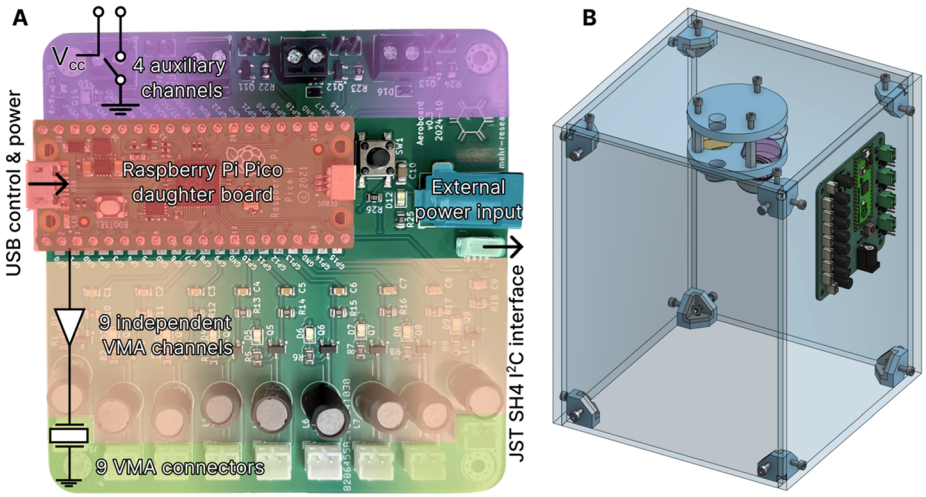

Fig. 9 The AeroBoard (A) and its integration into our aerosol reactor (B). Power can be supplied either *via* USB or externally for mean loads above 5 V and 1 A. Nine VMA drivers are connected to GPIOs 7–15 of the Raspberry Pi Pico daughter board, enabling fully synchronised control of VMA activations. An additional four GPIO pins (16–19) can be used for switching peripheral devices with the same synchronisation guarantees. A 4-pin JST SH format connector facilitates interfacing with I^2C devices, such as sensors. The reactor houses an array of reagent atomisers (two shown in this case) secured *via* a configurable 3D printed bracket. Each reagent module includes a glass vial with a piezoelectric VMA attached to the cap. A pair of wires (not shown) connects each VMA to one of the nine connectors on the AeroBoard, highlighted in green.

designed for programmable execution. In what follows, we will outline directions for future development in the area, including tackling limitations of the current implementation. Aerosol properties, critically size distribution, are known to have a strong dependence on relative humidity — and for non-aqueous solvents, solvent vapor pressure — which is not currently taken into account. Relying on short, isolated bursts of aerosol release, we have sought to minimize the change in relative humidity from ambient due to the evaporation of reagent solutions. In parallel, we are working on a reactor with closed-loop active humidity control that can maintain relative humidity at any desired level throughout the experiment. Visual inspection of microscope images relying solely on RGB values has been sufficient for validating this methodology, including with non-specialist camera set-ups,[20] but has limited the possibility to reason about reactivity in a quantitative manner. Hyperspectral imaging techniques, recently demonstrated in conjunction with microscopy,[21] can address this deficiency by enabling quantitative modelling of the effects of concentration and mixing. Moving beyond optical detection techniques, mass spectrometry provides access to much richer reactivity information. We envision interfacing with mass spectrometers directly *via* release of analytes to MS as aerosols, using a gas-phase soft ionisation technique such as atmospheric pressure chemical ionisation (APCI) to charge analyte molecules. There is also a growing set of techniques for MS imaging, *e.g.* desorption electrospray ionisation (DESI) capable of yielding composition data for individual droplets.

Representing experimental outcomes *via* the spatial distribution of final droplet compositions is a departure from the concise picture provided by yield figures in bulk synthesis. On the other hand, it gives access to a wealth of reactivity observations in parallel and without additional effort. The inherent variability in stoichiometry can be invaluable as it can reveal an array of possible products in a single experiment. Collected statistics can be used for reaction optimisation by changing the timing and duration of reagent pulses to maximise reactivity, especially useful in multi-step, multi-component reactions where temporal control of stoichiometry can influence product makeup. Exploiting the unique possibilities offered in this new probabilistic regime is dependent on the development of new computational frameworks to translate discovery/optimisation goals into strategies for fine-tuning the inputs to programmable aerosol reactors.

On the hardware front, activation of VMAs using with Gaussian or Lorentzian pulses has been demonstrated to result in a more uniform distribution of droplet sizes,[22] albeit at the expense of atomisation rate. Producing these bespoke waveforms could facilitate experiments with greater dependence on droplets of a specific diameter. Built-in automatic frequency tuning is another potential extension, allowing plug-and-play operation with a range of VMA form factors and solvents with widely varying physical properties. Finally, although the stochastic nature of reactivity in the aerosol phase reduces the emphasis on exact agreement between theoretical stoichiometry and dispensed amounts — as even with perfect dosing a wide range of stoichiometries are generated through random droplet collisions — direct reporting of dispensed amounts, *via* built-in sensing of liquid weight/pressure, will be valuable in the context of generating a reproducible product distribution for specific experimental regimes, notably at the optimisation stage.

Conclusion

While not a replacement for bulk synthesis, the aerosol medium presents exciting new possibilities for chemistry in the unfolding era of digitisation. It responds to the field's growing need for

experimental media fundamentally designed for programmable execution and rapid computational analysis. We hope that wider adoption of this experimental framework and the accompanying hardware platform will open the way for chemistry domain experts to explore the possibilities offered by aerosols as a reaction medium. Though we have used a conventional set of reactions for validating this methodology, its true potential lies in exploring the breadth of possible reaction products rather than obtaining a single product in high yield or purity. In line with this, we envision progress, initially in terms of adapting and optimising known procedures but increasingly leading to development of new protocols and procedures fundamentally discovered and optimised in an aerosol reactor.

Data availability

CAD files for all mechanical parts are freely available *via* the Onshape platform (**https://cad.onshape.com/documents/3974c62b9a8592129eaf9f65**). Experimental procedures for all experiments (encoded using the open-source CtrlAer library), along with analysis code for microscopy data (**https://github.com/MehrResearch/aerosol_synthesis**). Webpage for browsing the acquired images and image analysis outcomes (**https://mehrresearch.github.io/aerosol_synthesis/**). Hardware schematics and bill of materials for assembling the AeroBoard platform is available on GitHub (**https://github.com/MehrResearch/AeroBoard**). Microscope imaging data for all samples has been deposited online and is freely accessible *via* the Zenodo platform (**https://doi.org/10.5281/zenodo.15632556**).

Author contributions

Jakub D. Wosik: investigation, methodology, writing original draft (equal), validation. Chaoyi Zhu: investigation, methodology, writing original draft (equal), validation. Zehua Li: investigation, methodology, validation. S. Hessam M. Mehr: conceptualisation, methodology, software, validation, formal analysis, funding acquisition, project administration, supervision, visualisation, writing original draft (equal).

Conflicts of interest

The authors declare no conflicts of interest.

Acknowledgements

The authors would like to thank Professor Jonathan Reid, Dr Bryan Bzdek and Dr Joshua Harrison (School of Chemistry, University of Bristol) for fruitful discussions and for access to equipment at the Bristol Aerosol Research Centre (BARC). This project was supported by the Leverhulme Trust (Early Career Fellowship ECF-2021-298), the Royal Society of Chemistry (Research Enablement Grant E22-7895308996), and the University of Glasgow (Lord Kelvin–Adam Smith Leadership Fellowship).

References

1 M. Girod, E. I. Moyano, D. Campbell and R. Graham Cooks, Accelerated bimolecular reactions in microdroplets studied by desorption electrospray ionization mass spectrometry, *Chem. Sci.*, 2011, **2**(3), 501–510.
2 X. Yan, R. M. Bain and R. G. Cooks, Organic Reactions in Microdroplets: Reaction Acceleration Revealed by Mass Spectrometry, *Angew. Chem., Int. Ed.*, 2016, **55**(42), 12960–12972.
3 X. Song, C. Basheer and R. N. Zare, Making ammonia from nitrogen and water microdroplets, *Proc. Natl. Acad. Sci. U. S. A.*, 2023, **120**(16), e2301206120.
4 S. Banerjee, E. Gnanamani, X. Yan and R. N. Zare, Can all bulk-phase reactions be accelerated in microdroplets?, *Analyst*, 2017, **142**(9), 1399–1402.
5 C. F. Chamberlayne and R. N. Zare, Microdroplets can act as electrochemical cells, *J. Chem. Phys.*, 2022, **156**(5), 054705.
6 I. Nam, H. G. Nam and R. N. Zare, Abiotic synthesis of purine and pyrimidine ribonucleosides in aqueous microdroplets, *Proc. Natl. Acad. Sci. U. S. A.*, 2018, **115**(1), 36–40.
7 J. K. Lee, D. Samanta, H. G. Nam and R. N. Zare, Spontaneous formation of gold nanostructures in aqueous microdroplets, *Nat. Commun.*, 2018, **9**(1), 1562.
8 J. K. Lee, D. Samanta, H. G. Nam and R. N. Zare, Micrometer-Sized Water Droplets Induce Spontaneous Reduction, *J. Am. Chem. Soc.*, 2019, **141**(27), 10585–10589.
9 S. V. Ley and D. E. Fitzpatrick, Ingham RichardJ, Myers RM. Organic Synthesis: March of the Machines, *Angew. Chem., Int. Ed.*, 2015, **54**(11), 3449–3464.
10 L. Zhang and S. H. M. Mehr, In situ synthesis within micron-sized hydrogel reactors created *via* programmable aerosol chemistry, *Digital Discovery*, 2024, **3**(12), 2424–2433.
11 B. R. Bzdek, J. P. Reid and M. I. Cotterell, Open questions on the physical properties of aerosols, *Commun. Chem.*, 2020, **3**, 105.
12 B. Ahmed, D. Barrow and T. Wirth, Enhancement of Reaction Rates by Segmented Fluid Flow in Capillary Scale Reactors, *Adv. Synth. Catal.*, 2006, **348**(9), 1043–1048.
13 A. Lähde, I. Koshevoy, T. Karhunen, T. Torvela, T. A. Pakkanen and J. Jokiniemi, Aerosol-assisted synthesis of gold nanoparticles, *J. Nanopart. Res.*, 2014, **16**(11), 2716.
14 A. Fathi, M. Ahmadi, T. Madrakian, A. Afkhami and S. Asadi, A multi-nebulizer-based aerosol-assisted system for the synthesis of magnetic iron mixed metal oxides nanoparticles (MFe^2O^4, M = Fe^{2+}, Ni^{2+}, Mn^{2+}, Co^{2+}, Zn^{2+}), *Chem. Pap.*, 2023, **77**(11), 6933–6946.
15 J. Sun, H. T. Kwon and H. K. Jeong, Continuous synthesis of high quality metal–organic framework HKUST-1 crystals and composites *via* aerosol-assisted synthesis, *Polyhedron*, 2018, **153**, 226–233.
16 M. Mofidfar, M. A. Mehrgardi and R. N. Zare, Water Microdroplets Surrounded by Alcohol Vapor Cause Spontaneous Oxidation of Alcohols to Organic Peroxides, *J. Am. Chem. Soc.*, 2024, **146**(27), 18498–18503.

17 A. Kirillov, E. Mintun, N. Ravi, H. Mao, C. Rolland, L. Gustafson, *et al*, Segment Anything, in: *Proceedings of the IEEE/CVF International Conference on Computer Vision* [Internet], 2023 [cited 2024 Mar 25], pp., 4015–4026, **https://openaccess.thecvf.com/content/ICCV2023/html/Kirillov_Segment_Anything_ICCV_2023_paper.html**.
18 H. Mehr, MehrResearch/AeroBoard: v0.3.5, 2025.
19 S. H. M. Mehr, CtrlAer: Programmable real-time execution of scientific experiments using a domain specific language for the Raspberry Pi Pico/Pico 2, *SoftwareX*, 2025, **30**, 102175.
20 H. M. Jiang and S. H. Mehr, Detection of Micron-Sized Chemical Droplets Using a Commodity Digital Camera Setup, *ChemRxiv*, 2023, DOI: **10.26434/chemrxiv-2023-swkp8**, **https://chemrxiv.org/engage/chemrxiv/article-details/64f4ef5cdd1a73847f1d969a**.
21 L. Gao and R. T. Smith, Optical hyperspectral imaging in microscopy and spectroscopy – a review of data acquisition, *J. Biophotonics*, 2015, **8**(6), 441–456.
22 R. Kaimal, J. Feng, D. Halim, Y. Ren, V. L. Wong and K. H. Cheah, Impact of piezoelectric driving waveform on performance characteristics of vibrating mesh atomizer (VMA), *Exp. Therm. Fluid Sci.*, 2025, **160**, 111331.